

Explosion geometry of a rotating $13 M_{\odot}$ star driven by the SASI-aided neutrino-heating supernova mechanism

Yudai SUWA¹, Kei KOTAKE^{2,3}, Tomoya TAKIWAKI³, Stuart C. WHITEHOUSE⁴, Matthias LIEBENDÖRFER⁴, and Katsuhiko SATO^{5,6}

¹*Department of Physics, School of Science, The University of Tokyo, Tokyo 113-0033*

²*Division of Theoretical Astronomy, National Astronomical Observatory of Japan, Mitaka, Tokyo 181-8588, Japan*

³*Center for Computational Astrophysics, National Astronomical Observatory of Japan, Mitaka, Tokyo 181-8588, Japan*

⁴*Department of Physics, University of Basel, Klingelbergstr. 82, CH-4056 Basel, Switzerland*

⁵*The Institute for the Physics and Mathematics of the Universe, the University of Tokyo, Kashiwa, Chiba, 277-8568, Japan*

⁶*Department of Physics, School of Science and Engineering, Meisei University, 2-1-1 Hodokubo, Hino-shi, Tokyo 191-8506, Japan*

suwa@utap.phys.s.u-tokyo.ac.jp, suwa@yukawa.kyoto-u.ac.jp

(Received ; accepted)

Abstract

By performing axisymmetric hydrodynamic simulations of core-collapse supernovae with spectral neutrino transport based on the isotropic diffusion source approximation scheme, we support the assumption that the neutrino-heating mechanism aided by the standing accretion shock instability and convection can initiate an explosion of a $13 M_{\odot}$ star. Our results show that bipolar explosions are more likely to be associated with models which include rotation. We point out that models, which form a north-south symmetric bipolar explosion, can lead to larger explosion energies than for the corresponding unipolar explosions.

Key words: supernovae: general — hydrodynamics — neutrinos — instabilities

1. Introduction

Core-collapse supernovae have long attracted the attention of astrophysicists because they have many facets playing important roles in astrophysics. They herald the birth of neutron stars and black holes; they are a major site for nucleosynthesis; they influence galactic dynamics; they trigger further star formation and they are prodigious emitters of neutrinos and gravitational waves. Despite rigorous theoretical studies for more than 40 years, the details of the explosion mechanism have been obscured under the thick veils of massive stars.

For more than two decades, the neutrino-heating mechanism (Wilson 1985; Bethe & Wilson 1985), relying on the energy deposition via neutrinos behind the stalled shock, has been supposed as the most promising scenario. However, one important lesson we have learned from the work of Liebendörfer et al. (2001); Rampp & Janka (2002); Thompson et al. (2003); Sumiyoshi et al. (2005) is that the neutrino heating, albeit with the best input physics and numerics to date, fails in spherical symmetry (1D) (see, however, Kitaura et al. 2006).

Pushed by supernova observations of the blast morphology (e.g., Wang et al. 2001; Tanaka et al. 2007), it is now almost certain that the breaking of the spherical symmetry is the key to the supernova puzzle. The multi-dimensional (multi-D) hydrodynamic motion associated with convective overturn in the postshock region (Herant et al. 1994; Burrows et al. 1995; Janka & Mueller 1996; Fryer & Warren 2002; Fryer & Warren 2004) and the recently identified standing accretion shock insta-

bility (SASI) (e.g., Blondin et al. 2003; Scheck et al. 2004; Ohnishi et al. 2006; Foglizzo et al. 2007; Murphy & Burrows 2008; Iwakami et al. 2008; Iwakami et al. 2009; Guilet et al. 2009), are expected to help the neutrino-driven explosion mechanism. This is because the sojourn time of the accreting material in the gain region can be longer than in the 1D case, which enhances the efficiency of the energy deposition behind the stalled shock.

In fact, several explosion models have been reported recently in simulations that include multi-D effects that increase the neutrino heating (Buras et al. 2006; Marek & Janka 2009; Bruenn et al. 2009). Based on the long-term two-dimensional (2D) simulations with one of the best available neutrino transport approximations, Buras et al. (2006) firstly report an explosion for the non-rotating low-mass ($11.2 M_{\odot}$) progenitor of Woosley et al. (2002). Due to the compactness of the iron core ($\sim 1.26 M_{\odot}$) with its steep outer density gradient, the explosion is initiated at ~ 300 ms after core bounce. This is much earlier than in Marek & Janka (2009), who observe the delayed onset of the explosion ~ 600 ms for a $15 M_{\odot}$ progenitor of Woosley & Weaver (1995) with a moderately rapid rotation imposed. Although the explosion mechanism by neutrino-heating is very plausible, there are other possible mechanisms, in which the magnetohydrodynamic (MHD) mechanism is included (see references in Kotake et al. 2006; Obergaulinger et al. 2006; Burrows et al. 2007b; Takiwaki et al. 2009). Another suggested mechanism relies on acoustic energy deposition via oscillating proton-neutron stars (PNSs), which has been discovered by a series of 2D multi-energy flux-limited-diffusion transport

simulations (Burrows et al. 2006; Burrows et al. 2007a). Although the additional energy input from sound appears to be robust enough to explode even the most massive progenitors (Burrows et al. 2007a), it remains a matter of vivid debate and has yet to be confirmed by other groups. Also exotic physics in the core of the PNS may have a potential to trigger explosions (e.g., Sagert et al. 2009).

In this *Letter*, we present axisymmetric explosion models for a $13 M_{\odot}$ progenitor model of Nomoto & Hashimoto (1988) in support of the theory that neutrino-heating aided by multi-D effects is able to cause supernova explosions. We choose the progenitor with a smaller iron core ($\sim 1.20 M_{\odot}$), anticipating an explosion since the progenitor mass lies between $11.2 M_{\odot}$ (Buras et al. 2006) and $15 M_{\odot}$ (Marek & Janka 2009). We perform 2D core-collapse simulation with spectral neutrino transport by the isotropic diffusion source approximation (IDSA) scheme currently developed by Liebendörfer et al. (2009). By comparing four exploding models with and without rapid rotation to one non-exploding 1D model, we point out that models that produce a north-south symmetric bipolar explosion can lead to larger explosion energies than for the corresponding unipolar explosions. Our results show that the explosion geometry is more likely to be bipolar in models that include rotation.

2. Numerical Methods and Models

Our 2D simulations are performed using a newly developed code which implements spectral neutrino transport using the IDSA scheme (Liebendörfer et al. 2009) in a ZEUS-2D code (Stone & Norman 1992). Following the spirit of the so-called ray-by-ray approach, the IDSA scheme further splits the neutrino distribution into two components, both of which are solved using separate numerical techniques. Although it does not yet include heavy lepton neutrinos such as ν_{μ}, ν_{τ} ($\bar{\nu}_{\mu}, \bar{\nu}_{\tau}$) and the inelastic neutrino scattering with electron, the innovative approach taken in the scheme saves a significant amount of computational time compared to the canonical Boltzmann solvers (see Liebendörfer et al. 2009 for more details). Expecting a bigger chance to produce explosions (Marek & Janka 2009), we employ the soft equation of state (EOS) by Lattimer & Swesty (1991) with a compressibility modulus of $K = 180$ MeV. The self gravity is implemented by solving the Poisson equation by the Modified Incomplete Cholesky Conjugate Gradient (MICCG) method (Kotake et al. 2003), but without relativistic corrections.

The simulations are performed on a grid of 300 logarithmically spaced radial zones up to 5000 km. To test the sensitivity with respect to angular resolution, the grid is varied to consist of 64 or 128 equidistant angular zones covering $0 \leq \theta \leq \pi$. For the neutrino transport, we use 20 logarithmically spaced energy bins reaching from 3 to 300 MeV.

All supernova calculations in this work are based on the $13 M_{\odot}$ model by Nomoto & Hashimoto (1988). The computed models are listed in the first column of Table 1, in which one calculation (model M13-1D) is conducted

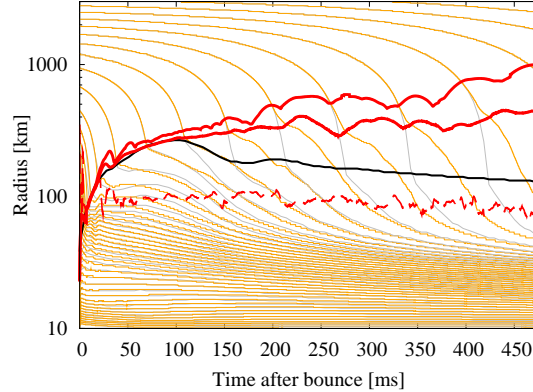


Fig. 1. Time evolution of Models M13-1D and M13-2D, visualized by mass shell trajectories in thin gray and orange lines, respectively. Thick lines in red (for model M13-2D) and black (model M13-1D) show the position of shock waves, noting for 2D that the maximum (top) and average (bottom) shock position are shown. The red dashed line represents the position of the gain radius, which is similar to the 1D case (not shown).

in spherical symmetry. Other models are 2D simulations with or without rotation (indicated by rot) with different numerical resolution in the lateral direction (64 or 128, denoted by "hr" (high resolution) in Table 1). For the rotating models, we impose rotation on the progenitor core with initially a constant angular frequency of $\Omega_0 = 2$ rad/s inside the iron core with a dipolar cut off ($\propto r^{-2}$) outside, which corresponds to $\beta \sim 0.18\%$ with β being the ratio of the rotational to the gravitational energy. This rotation rate is fairly large and may lead to a spiral mode of the SASI (Yamasaki & Foglizzo 2008). In addition, this strong rotation may induce a strong magnetic field due to winding and the magneto-rotational instability and produce a jet-like outflow (Kotake et al. 2006). Although these effects could modify the dynamics of the postbounce phase, the approximate treatment in this study (axisymmetry without magnetic fields) does not allow us to investigate them in this article.

3. Results

Figure 1 depicts the difference between the time evolutions of model M13-1D (thin gray lines) and model M13-2D (thin orange lines), visualized by mass shell trajectories. Until ~ 100 ms after bounce, the shock position of the 2D model (thick red line) is similar to the 1D model (thick black line). Later on, however, the shock for model M13-2D does not recede as for M13-1D, but gradually expands and reaches 1000 km at about 470 ms after bounce. Comparing the position of the gain radius (red dashed line) to the shock position of M13-1D (thick black line) and M13-2D (thick red line), one can see that the advection time of the accreting material in the gain region can be longer in 2D than 1D. This longer exposure of cool matter in the heating region to the irradiation of hot outstreaming neutrinos from the PNS is essential for the increased efficiency of the neutrino heating in multi-D

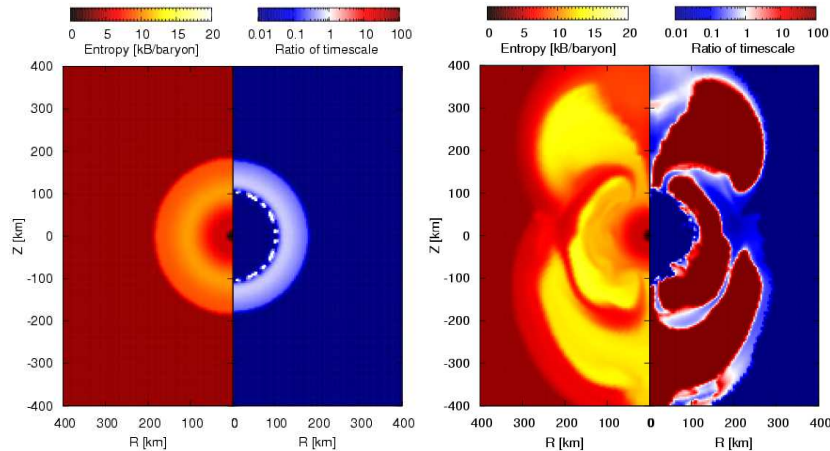


Fig. 2. Snapshot of the distribution of entropy (left half) and the ratio of the advection to the heating timescale (right half) for models of M13-1D (left) and M13-2D (right) at 200 ms after bounce.

models.

A more detailed analysis of the timescale is shown in Figure 2. The right-half shows $\tau_{\text{adv}}/\tau_{\text{heat}}$, which is the ratio of the advection to the neutrino heating timescale. For the 2D model (right panel), it can be shown that the condition of $\tau_{\text{adv}}/\tau_{\text{heat}} \gtrsim 1$ is satisfied behind the aspherical shock, which is deformed predominantly by the SASI, while the ratio is shown to be smaller than unity in the whole region behind the spherical standing accretion shock (left panel:1D). Note that τ_{heat} is estimated locally by e_{bind}/Q_{ν} , where e_{bind} is the local specific binding energy (the sum of internal plus kinetic plus gravitational energies) and Q_{ν} is the specific heating rate by neutrinos, and that τ_{adv} is given by $[r - r_{\text{gain}}(\theta)]/|v_r(r, \theta)|$, where r_{gain} is the gain radius and v_r is the radial velocity. Comparing the left-half of each panel, the entropy for the 2D model is shown to be larger than for the 1D model. This is also the evidence that the neutrino heating works more efficiently in multi-D.

We now move on to discuss models with rotation. Both, for model M13-rot and its high resolution counterpart, model M13-rot-hr, we obtain neutrino-driven explosions (see, t_{1000} and E_{dia} in Table 1). The rapid rotation chosen for this study mainly affects the explosion dynamics in the postbounce phase, which we will discuss in the following.

For the rotating model, the dominant mode of the shock deformation after bounce is almost always the $\ell = 2$ mode although the $\ell = 1$ mode can be as large as the $\ell = 2$ mode when the SASI enters the non-linear regime ($\gtrsim 200$ ms after bounce). In contrast to this rotation-induced $\ell = 2$ deformation, the $\ell = 1$ mode tends to be larger than the $\ell = 2$ mode for the 2D models without rotation in the saturation phase. As shown in Figure 3, this leads to different features in the shock geometry, namely the preponderance of the unipolar explosion for the 2D models without rotation (left), and the bipolar (north-south symmetric) explosion with rotation (right).

Since it is impossible to calculate precise explosion energies at this early stage, we define a *diagnostic* energy that refers to the integral of the energy over all zones that have

a positive sum of the specific internal, kinetic and gravitational energy. Figure 4 shows the comparison of the diagnostic energies for the 2D models with and without rotation. Although the diagnostic energies depend on the numerical resolutions quantitatively, they show a continuous increase for the rotating models. The diagnostic energies for the models without rotation, on the other hand, peak around 180 ms when the neutrino-driven explosion sets in (see also Figure 1), and show a decrease later on. With values of order 10^{49} erg it is not yet clear whether these models will also eventually lead to an explosion.

The reason for the greater explosion energy for models with rotation is due to the bigger mass of the exploding material. This is because the north-south symmetric ($\ell = 2$) explosion can expel more material than for the unipolar explosion. In fact, the mass enclosed inside the gain radius is shown to be larger for the rotating models (e.g., Table 1). The explosion energies when we terminated the simulation are less than $\lesssim 10^{50}$ erg for all the models. For the rotating models, we are tempted to speculate that they could become as high as $\sim 10^{51}$ erg within the next 500 ms by a linear extrapolation. However, in order to unquestionably identify the robust feature of an explosion in the models, a longer-term simulation with improved input physics would be needed.

Our numerical results are qualitatively consistent with the results of Marek & Janka (2009) in the sense that in a relatively early postbounce phase the model with rotation shows a more clear trend of explosion than for the non-rotating models.

4. Summary and Discussion

By performing 2D core-collapse simulations of a $13 M_{\odot}$ star with spectral neutrino transport via the isotropic diffusion source approximation, we have found a strong dependence of the expansion of the shock radius and the likelihood for an explosion on the initial rotation rate. In all cases the shock is driven outward by the neutrino heating mechanism aided by multi-D effects such as the SASI

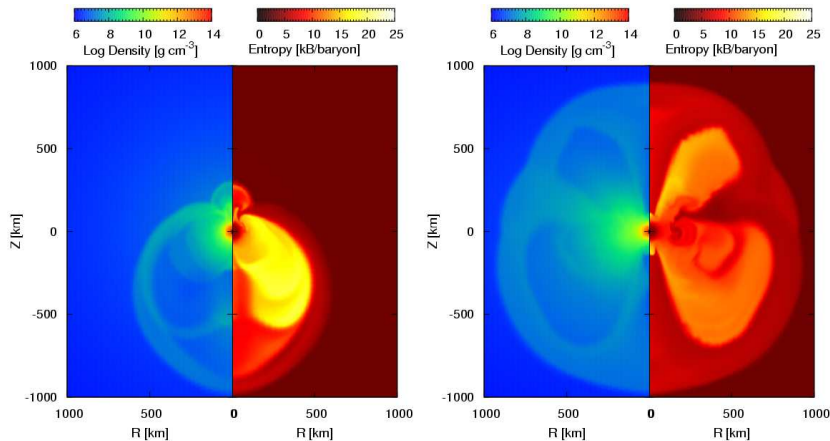


Fig. 3. Snapshots of the density (left half) and the entropy (right half) for models M13-2D (left) and M13-rot (right) at the epoch when the shock reaches 1000 km, corresponding to ~ 470 ms after bounce in both cases.

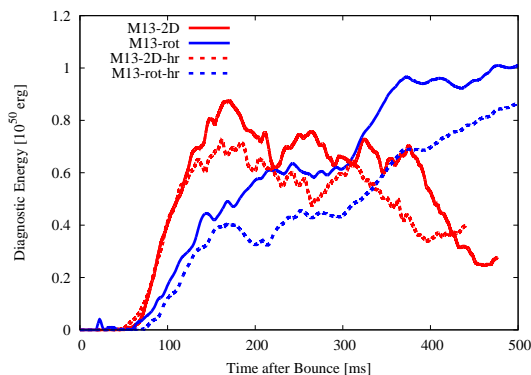


Fig. 4. Time evolution of the diagnostic energy versus post-bounce time for 2D models with and without rotation.

and convection. We have shown the preponderance of an bipolar explosion for 2D models with rotation. We have pointed out that the explosion energy can become larger for models with bipolar explosions.

The conclusion with respect to the effects of rotation obtained in this study differs from that of Marek & Janka (2009), who suggested that the rotation has a negative impact on the explosion. They obtained the expansion of the shock wave only for the rotating model (M15LS-rot), while the nonrotating model did not show an expansion due to the short simulation time (see Fig. 6 in their paper). Therefore they could not compare the expanding shock evolution in both the rotating and the nonrotating cases so that their discussion is limited to the shock oscillation phase.

Here it should be noted that the simulations in this paper are only a very first step towards more realistic supernova models (e.g., Marek & Janka 2009; Burrows et al. 2007a; Bruenn et al. 2009). The approximations adopted in this paper should be improved, for example the omission of heavy lepton neutrinos, the inelastic neutrino scattering, and the ray-by-ray approach. The former two, may act to suppress the explosion. However we think that qualitative effects induced by rotation will not

be affected so much because they are produced mainly by the hydrodynamic interplay of the SASI and the rotation. The ray-by-ray approach may lead to the overestimation of the directional dependence of the neutrino anisotropies (see discussions in Marek & Janka 2009). On the other hand, the lateral neutrino emission and the enhanced heating near the polar regions, such as from the oblately deformed protoneutron star due to rapid rotation (e.g., Kotake et al. 2003), could be underestimated. Apparently the full-angle transport will give us the correct answer (e.g., Ott et al. 2008). In addition, due to the coordinate symmetry axis, the SASI develops preferentially along the axis, thus it could provide a more favorable condition for the explosion. As several exploratory simulations have been done recently (Iwakami et al. 2008; Scheidegger et al. 2008; Iwakami et al. 2009), 3D supernova models are indeed necessary.

Bearing these caveats in mind, the role of rotation acting on the neutrino-driven explosions, is qualitatively new. Yet there remain a number of issues to be studied. We have to clarify the progenitor dependence and also investigate the effects of rotation more systematically by changing its strength in a parametric manner (possibly with magnetic fields). It will be interesting to study the neutrino and gravitational-wave signals. This paper is a prelude for the forthcoming work that will clarify these issues one by one.

Y.S would like to thank to E. Müller and H.-Th. Janka for their kind hospitality during his stay in MPA. K.K is grateful to S. Yamada for continuing encouragements. Numerical computations were in part carried on XT4 at CfCA of the National Astronomical Observatory of Japan. S.C.W and M.L are supported by the Swiss National Science Foundation under grant No. PP00P2-124879 and 200020-122287. This study was supported in part by the Japan Society for Promotion of Science (JSPS) Research Fellowships (YS) and the Grants-in-Aid for the Scientific Research from the Ministry of Education, Science and Culture of Japan (Nos. 19540309 and 20740150).

Table 1. Model summary

Models	Dimension	Ω_0 [rad/s]	N_θ	t_{1000} [ms]	E_{dia} [10^{50} erg]	M_{gain} [M_\odot]
M13-1D	1D	–	1	–	–	–
M13-2D	2D	–	64	470	0.26	0.017
M13-rot	2D & rotation	2	64	480	0.95	0.067
M13-2D-hr	2D	–	128	420	0.40	0.018
M13-rot-hr	2D & rotation	2	128	520	0.78	0.060

Ω_0 is the precollapse angular velocity. N_θ represents the lateral grid number covering $0 \leq \theta \leq \pi$. “hr (high resolution)” indicates the runs for $N_\theta = 128$. t_{1000} represents the time (measured after bounce) when the average shock radius becomes 1000 km. E_{dia} is the diagnostic energy defined as the total energy (internal plus kinetic plus gravitational), integrated over all matter where the sum of the corresponding specific energies is positive. M_{gain} is the mass inside the gain layer. The latter quantities are given at 450 ms postbounce.

References

- Bethe, H. A. & Wilson, J. R. 1985, *ApJ*, 295, 14
- Blondin, J. M., Mezzacappa, A., & DeMarino, C. 2003, *ApJ*, 584, 971
- Bruenn, S. W., Mezzacappa, A., Hix, W. R., Blondin, J. M., Marronetti, P., Messer, O. E. B., Dirk, C. J., & Yoshida, S. 2009, *Journal of Physics Conference Series*, 180, 012018
- Buras, R., Janka, H., Rampp, M., & Kifonidis, K. 2006, *A&A*, 457, 281
- Burrows, A., Hayes, J., & Fryxell, B. A. 1995, *ApJ*, 450, 830
- Burrows, A., Livne, E., Dessart, L., Ott, C. D., & Murphy, J. 2006, *ApJ*, 640, 878
- . 2007a, *ApJ*, 655, 416
- . 2007b, *ApJ*, 664, 416
- Foglizzo, T., Galletti, P., Scheck, L., & Janka, H. 2007, *ApJ*, 654, 1006
- Fryer, C. L. & Warren, M. S. 2002, *ApJL*, 574, L65
- . 2004, *ApJ*, 601, 391
- Gillet, J., Sato, J., & Foglizzo, T. 2009, *ArXiv:0910.3953*
- Herant, M., Benz, W., Hix, W. R., Fryer, C. L., & Colgate, S. A. 1994, *ApJ*, 435, 339
- Iwakami, W., Kotake, K., Ohnishi, N., Yamada, S., & Sawada, K. 2008, *ApJ*, 678, 1207
- . 2009, *ApJ*, 700, 232
- Janka, H. & Mueller, E. 1996, *A&A*, 306, 167
- Kitaura, F. S., Janka, H., & Hillebrandt, W. 2006, *A&A*, 450, 345
- Kotake, K., Sato, K., & Takahashi, K. 2006, *Rep. Prog. Phys.*, 69, 971
- Kotake, K., Yamada, S., & Sato, K. 2003, *ApJ*, 595, 304
- Lattimer, J. M. & Douglas Swesty, F. 1991, *Nuclear Physics A*, 535, 331
- Liebendörfer, M., Mezzacappa, A., Thielemann, F.-K., Messer, O. E., Hix, W. R., & Bruenn, S. W. 2001, *Phys. Rev. D*, 63, 103004
- Liebendörfer, M., Whitehouse, S. C., & Fischer, T. 2009, *ApJ*, 698, 1174
- Marek, A. & Janka, H. 2009, *ApJ*, 694, 664
- Murphy, J. W., & Burrows, A. 2008, *ApJ*, 688, 1159
- Nomoto, K. & Hashimoto, M. 1988, *Phys. Rep.*, 163, 13
- Obergaulinger, M., Aloy, M. A., & Müller, E. 2006, *A&A*, 450, 1107
- Ohnishi, N., Kotake, K., & Yamada, S. 2006, *ApJ*, 641, 1018
- Ott, C. D., Burrows, A., Dessart, L., & Livne, E. 2008, *ApJ*, 685, 1069
- Ott, C. D., Burrows, A., Thompson, T. A., Livne, E., & Walder, R. 2006, *ApJS*, 164, 130
- Rampp, M. & Janka, H. 2002, *A&A*, 396, 361
- Sagert, I., Fischer, T., Hempel, M., Pagliara, G., Schaffner-Bielich, J., Mezzacappa, A., Thielemann, F.-K., & Liebendörfer, M. 2009, *Physical Review Letters*, 102, 081101
- Scheck, L., Plewa, T., Janka, H., Kifonidis, K., & Müller, E. 2004, *Physical Review Letters*, 92, 011103
- Scheidegger, S., Fischer, T., Whitehouse, S. C., & Liebendörfer, M. 2008, *A&A*, 490, 231
- Stone, J. M. & Norman, M. L. 1992, *ApJS*, 80, 753
- Sumiyoshi, K., Yamada, S., Suzuki, H., Shen, H., Chiba, S., & Toki, H. 2005, *ApJ*, 629, 922
- Suwa, Y. *et al.* 2010, in prep.
- Takiwaki, T., Kotake, K., & Sato, K. 2009, *ApJ*, 691, 1360
- Tanaka, M., Maeda, K., Mazzali, P. A., & Nomoto, K. 2007, *ApJL*, 668, L19
- Thompson, T. A., Burrows, A., & Pinto, P. A. 2003, *ApJ*, 592, 434
- Wang, L., Howell, D. A., Höflich, P., & Wheeler, J. C. 2001, *ApJ*, 550, 1030
- Wilson, J. R. 1985, in *Numerical Astrophysics*, ed. J. M. Centrella, J. M. Leblanc, & R. L. Bowers, 422
- Woosley, S. E., Heger, A., & Weaver, T. A. 2002, *Reviews of Modern Physics*, 74, 1015
- Woosley, S. E. & Weaver, T. A. 1995, *ApJS*, 101, 181
- Yamasaki, T., & Foglizzo, T. 2008, *ApJ*, 679, 607